The Astrophysical Journal, 846:148 (8pp), 2017 September 10 https://doi.org/10.3847/1538-4357/aa85e0

Production of Sulfur Allotropes in Electron Irradiated Jupiter Trojans Ice Analogs

Ahmed Mahjoub[1], Michael J. Poston[1,2], Jordana Blacksberg[1], John M. Eiler[2], Michael E. Brown[2], Bethany L. Ehlmann[1,2], Robert Hodyss[1], Kevin P. Hand[1], Robert Carlson[1], and Mathieu Choukroun[1]

[1] Jet Propulsion Laboratory, California Institute of Technology, Pasadena, CA 91109, USA; Mahjoub.Ahmed@jpl.nasa.gov

[2] California Institute of Technology, Division of Geological and Planetary Sciences, Pasadena, CA 91125, USA

Received 2017 May 13; revised 2017 August 1; accepted 2017 August 8; published 2017 September 12

Abstract

In this paper, we investigate sulfur chemistry in laboratory analogs of Jupiter Trojans and Kuiper Belt Objects (KBOs). Electron irradiation experiments of CH_3OH–NH_3–H_2O and H_2S–CH_3OH–NH_3–H_2O ices were conducted to better understand the chemical differences between primordial planetesimals inside and outside the sublimation line of H_2S. The main goal of this work is to test the chemical plausibility of the hypothesis correlating the color bimodality in Jupiter Trojans with sulfur chemistry in the incipient solar system. Temperature programmed desorption (TPD) of the irradiated mixtures allows the detection of small sulfur allotropes (S_3 and S_4) after the irradiation of H_2S containing ice mixtures. These small, red polymers are metastable and could polymerize further under thermal processing and irradiation, producing larger sulfur polymers (mainly S_8) that are spectroscopically neutral at wavelengths above 500 nm. This transformation may affect the spectral reflectance of Jupiter Trojans in a different way compared to KBOs, thereby providing a useful framework for possibly differentiating and determining the formation and history of small bodies. Along with allotropes, we report the production of organo-sulfur molecules. Sulfur molecules produced in our experiment have been recently detected by *Rosetta* in the coma of 67P/Churyumov–Gerasimenko. The very weak absorption of sulfur polymers in the infrared range hampers their identification on Trojans and KBOs, but these allotropes strongly absorb light at UV and Visible wavelengths. This suggests that high signal-to-noise ratio UV–Vis spectra of these objects could provide new constraints on their presence.

Key words: astrochemistry – Kuiper belt: general – methods: laboratory: molecular – molecular processes – techniques: imaging spectroscopy

1. Introduction

Small bodies are the legacy left from the building blocks that accreted to create planets in the early solar system. Studying small objects such as Jupiter Trojans and Kuiper Belt Objects (KBOs) provides a unique perspective on the chemical and dynamical processes that shaped the solar system and a particular opportunity to evaluate new ideas about the formation and dynamical evolution of the solar system. In the framework of the Nice model, KBOs and Trojans are thought to have formed in the primordial planetesimal disk in the nascent solar system, with progenitors sourced from the same regions of the disk (Morbidelli et al. 2005; Nesvorny et al. 2013). As a result of dynamical instability and migration of giant planets, objects among this primordial disk of debris were dispersed, giving rise to the Jupiter Trojans and KBOs in their current positions, as well as other small objects. One of the most tantalizing properties of these two populations is the color bimodality of visible/near-infrared spectral slopes observed in both of them. Two classes of Trojans are distinctly identified by telescopic observations and referred to as red (R) and less red (LR) (Emery et al. 2011). A dynamical sub-population within the KBO family ("hot" KBOs) shows two sub-populations referred to as very red (VR) and red (R) KBOs (Brown et al. 2011; Wong & Brown 2016, 2017). This similarity in spectral slope bimodality is in accordance with a common origin for these two groups of objects. Moreover, the size distributions of Trojans and hot KBOs are consistent with each other, which supports the idea of a shared formation location (Fraser et al. 2014).

Surfaces of icy, airless bodies are exposed to photons and energetic particles from the Sun. This space weathering is believed to be responsible for the growth of organic-bearing refractory mantles on the surfaces of small icy bodies. There are increasing indications that organic polymers are present in primitive bodies in the solar system. For example, such refractory materials are considered to be a good spectral analog for the 3.2 μm band observed at the surface of comet 67P/Churyumov–Gerasimenko, hereafter 67P, by the VIRTS/*Rosetta* spectrometer (Quirico et al. 2016). These complex macromolecular organic materials are believed to play an important role in the red spectral slopes observed in small bodies in the solar system (Gradie & Veverka 1980) and are included in spectral modeling of Trojans (Emery et al. 2011). In one hypothesis, the bimodality in colors could be a result of differing ice compositions between the two populations. The retention of volatiles on the surface of objects in the outer primordial planetesimal disk depends on their orbital distances. Using a volatile loss model, Wong & Brown (2016) found that the stability line of H_2S passes through the region of the primordial disk, splitting objects into two groups: with sulfur and without sulfur. They used this location-dependent surface composition to propose a hypothesis explaining the surface color bimodality observed today for Trojans and KBOs as result of sulfur chemistry. This hypothesis is relevant only to small KBOs.

Small sulfur allotropes strongly absorb in the UV–Vis range, and the absorption wavelengths depend on the chain length (Meyer 1976). Meyer (1976) showed that the absorption of sulfur chains in UV–Vis range shifts toward high wavelengths with increasing numbers of S atoms, and reach an asymptote at 800 nm for chains containing five S atoms or more. Small

allotropes exhibit high degrees of temperature and irradiation instability. A direct test of the thermal polymerization of small sulfur allotropes was performed by Brabson et al. (1991). In their study, Brabson et al. (1991) applied a microwave discharge in sulfur vapor and condensed the obtained gas at 12 K. Using infrared spectroscopy coupled with isotopic shift analysis they convincingly concluded that the samples produced are mainly composed of S_2, S_3, and S_4, with less abundance of higher sulfur chains. Annealing these samples results in a decrease of allotrope bands and an increase in bands assigned to larger cyclic sulfur molecules.

It is well established that melting a sulfur powder at temperatures higher than 250°C modifies its color from yellow to red. By using UV–Vis spectroscopy, Meyer et al. (1971) attributed this change in color to the formation of allotropes. Cooling the liquid down to 70 K, does not change the color of the sample, which is interpreted as a preservation of sulfur allotropes at this temperature. Warming the sample from 70 K to room temperature changes the color of the sample to its original color: yellow. This has been interpreted as a consequence of the polymerization of unstable small sulfur chains to orthorhombic S_8. Similar observations were made after irradiation and thermal processing of S_2O ice samples (Baklouti et al. 2008). In Baklouti et al. (2008), the change of color from red to yellow is accompanied by the appearance of IR bands due to polysulfuroxide.

To gain insight into the role of H_2S on chemical and spectral properties of small primitive objects, we have conducted laboratory experiments testing the influence of sulfur chemistry on spectral slope in the visible–NIR range when it is added to a C-, N-, and O-bearing ice mixture. Mixed ices H_2S–CH_3OH–NH_3–H_2O "with H_2S" and CH_3OH–NH_3–H_2O "without H_2S" have been irradiated with a 10 keV electron beam and subsequently warmed to room temperature. First results show that the addition of sulfur strongly affects the slope in the Vis–NIR spectral range (M. J. Poston et al. 2017, in preparation). We have previously reported that adding H_2S leads to a significant change in the chemistry induced by electron irradiation (Mahjoub et al. 2016). Multiple sulfurous radiation products were detected, but all of them are transparent in the visible–NIR spectral range and cannot explain the observed reddening caused by the presence of sulfur in the initial ice samples. Here, we present new results supporting the formation of sulfur allotropes in the "with H_2S" samples. Contrasting the Temperature Programmed Desorption (TPD) curves of samples "with H_2S" against samples "without H_2S" permits the detection of S_2, S_3, S_4, and CH_3–S–CH_3, CH_3–S_2–CH_3, CH_3–SO_2–CH_3. The implication of this sulfur chemistry on the colors of Jupiter Trojans and KBOs, and the bimodality in spectral slopes of these two groups, is discussed.

This paper is structured as follows. In Section 2 we describe the experimental procedure. Our results are presented in Section 3. The astrophysical implications of this research are discussed in Section 4.

2. Experimental Methodology

Electron irradiation experiments were carried out using the Icy Worlds Simulation Laboratory at the Jet Propulsion Laboratory. A detailed description of the facilities and the capabilities of this laboratory can be found in Hand & Carlson (2011). The experimental setup consisted of a high-vacuum stainless steel chamber pumped by a Varian Turbo and backed by oil-free pumps (pressure after overnight pumping about 1×10^{-8} torr). The ices were vapor-deposited on a substrate attached to the cold finger of a closed-cycle helium cryostat (ARS model DE-204). An external manifold was used to prepare gas mixtures prior to deposition. The ice film was grown by leaking the gas mixture into the chamber and forming ices on the substrate, which was held at 50 K. Most of the gas deposited directly, but a small fraction did not, resulting in a rise of chamber pressure of a few 10^{-8} torr. High-energy electrons (10 keV) were directed at the ice with a typical beam current of 0.5 μA. All studied ices were submitted to the same fluence of electron energy $\sim 2 \times 10^{21}$ eV cm^{-2}. Radiation fluences were scaled to the outer-solar system based on the electron flux at 1 au, which was deduced from values given in Bennett et al. (2013). We found that the total fluence received by our ice samples corresponds to a timescale of 0.2 Myr for an object at 5 au and 1.8 Myr at 15 au. In the present work we focus our discussion on electron and thermal processing of H_2S–CH_3OH–NH_3–H_2O (3:3:3:1) "with H_2S" and CH_3OH–NH_3–H_2O (3:3:1) "without H_2S" mixed ices, which are expected for ices in KBOs and Trojans. As discussed in Mahjoub et al. (2016), the chemical composition of ice films calculated using infrared spectra and bond strengths of deposited molecules is different from the gas phase mixture. The compositions of the ices as estimated from the respective column densities are: CH_3OH–NH_3–H_2O = 73:12:15 for the "without H_2S " ice and H_2S–CH_3OH–NH_3–H_2O = 7:35:17:41 for the "with H_2S" sample. After irradiation for 19 hr at 50 K, samples were warmed to 120 K at 0.5 K minute^{-1} and held there for 1 additional hour under continued electron irradiation. After the electron irradiation was concluded, the samples were warmed at 0.5 K minute^{-1} to 300 K. This experimental procedure was chosen to simulate the irradiation and heating history of an icy surface scattered from the primordial Kuiper Belt region to the Jupiter Trojans region. The chemical evolution of the ice was monitored with a Midac Fourier transform infrared spectrometer covering a wavenumber range 400–7000 cm^{-1} at 2 cm^{-1} resolution. with 1024 scans accumulated. The angle of incidence of the infrared beam was ~16° to the normal of the ice film. The ice film was not optically thick: infrared light passed through the ice film and was reflected back through the film by the gold mirror to the detector, where the intensity measured was divided by the intensity of reflected light from the gold mirror alone, the spectrum of which was collected just prior to the ice deposition process. The thickness of the ice films has been estimated to between 1 and 2 μm (Mahjoub et al. 2016).

The TPD technique is widely used to study chemistry in irradiated ices for application to interstellar medium and solar system icy bodies. A Stanford Research Systems RGA 200 quadrupole mass spectrometer was used to monitor the gaseous species released when the irradiated ices were warmed. The mass spectrometer operated with a 70 eV electron impact ionization method scanning *m/z* 1–200. TPD spectra correspond to the measurement of masses of molecular species released over the temperature range 50–300 K. The comparison between species desorbed from the samples "with H_2S" and "without H_2S" helps the assignment of masses observed in RGA mass spectra to specific molecular species.

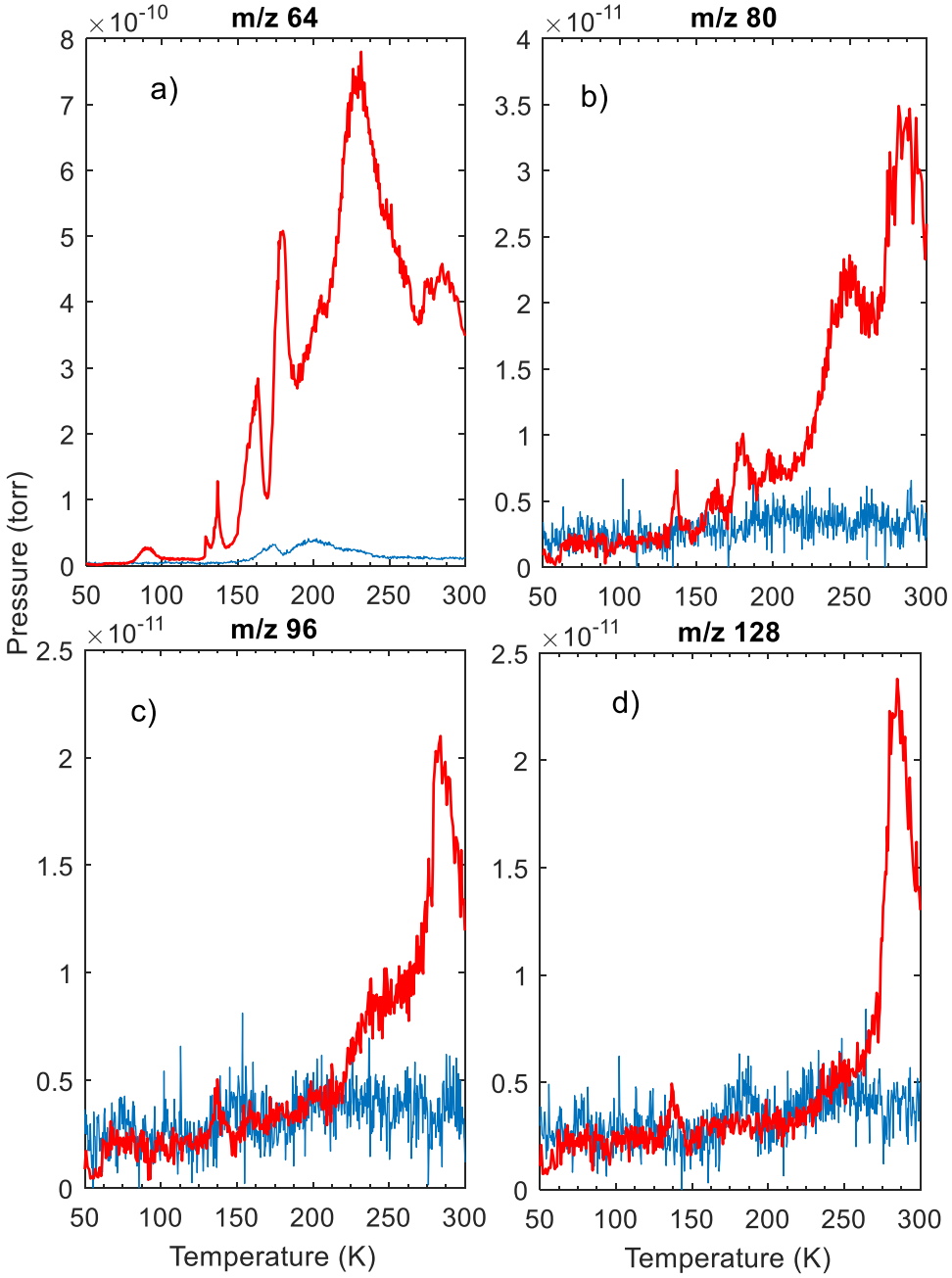

Figure 1. TPD curves corresponding to the irradiated "with H_2S" (red curves) and "without H_2S" (blue curves) experiments. Essentially no features are seen in the "without H_2S" TPD data. The ion currents at *m/z* 64, 96, and 128 correspond, respectively, to S_2+SO_2, S_3, and S_4. A possible assignment for mass 80 is S_2O+SO_3.

3. Results

All the sulfur-bearing molecules detected via infrared spectroscopy by Mahjoub et al. (2016) are confirmed by TPD measurements: OCS, SO, SO_2, CS, CS_2. For brevity, we present here only newly detected molecules. Figure 1 shows TPD curves of irradiated ice mixtures "with H_2S" and "without H_2S" recorded for *m/z* 64, 80, 96, and 128. For all these masses, a significant signal is detected only in the samples "with H_2S," which constrains the assignment of these masses to molecules containing at least one S atom. The mass *m/z* 64 can be assigned to either SO_2 or S_2. SO_2 has been detected by mid-IR spectroscopy in the samples "with H_2S" (Mahjoub et al. 2016).

To find out if SO_2 alone is responsible for the signal at *m/z* 64, we compare the TPD spectra of *m/z* 64 and *m/z* 48, corresponding to SO, the principle fragment of SO_2 (Figure 2). Figure 2 also presents a comparison between TPD curves at *m/z* 48 for the "with H_2S" and "without H_2S" samples. A significant signal is observed only from the "with H_2S" sample, indicating that this mass is mostly likely due to sulfur-containing molecules.

Mass 48 corresponds to the sulfur monoxide molecule, SO, which could be directly desorbed from the irradiated sample, or could be a product of fragmentation of SO_2, S_2O, and/or SO_3. CH_3SH could also be produced in our samples and would contribute to the signal at *m/z* 48. Deconvolution of contributions from all these possible candidates to mass 48 is not possible with these data. However, since S_2 does not produce

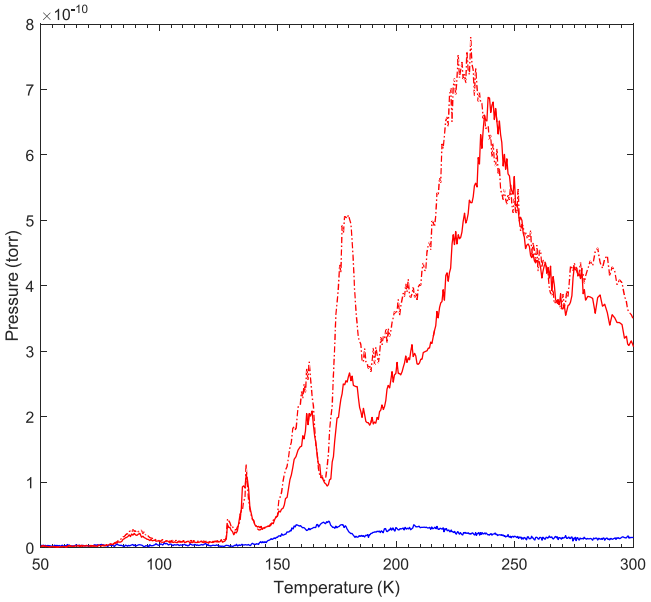

Figure 2. TPD curves at *m/z* 48 corresponding to the irradiated "with H_2S" (red solid curve) and "without H_2S" (blue curve) experiments and at *m/z* 64 (dashed red curve) for the "with H_2S" experiment.

fragments at mass 48, comparison between mass 64 and 48 (Figure 2) provides information on the likelihood that S_2 is present. At some temperatures the two peaks move synchronously, but at 230–240 K the two signals reach maxima with a separation of 9 K. This shift indicates that the two masses are decoupled at this temperature, which indicates that the desorption at $T = 230$ K could be due to other molecules in addition to SO_2. While these observations are circumstantial evidence of the possible formation of S_2 in the irradiated "with H_2S" sample, they are not enough for an actual detection.

Figure 3 compares TPD curves at *m/z* 64 and *m/z* 68, corresponding to $^{34}S_2$ isotopomer of S_2. It is unlikely that mass 68 corresponds to $S^{18}O_2$ since the natural abundance of ^{18}O is very low (0.2%) compared to ^{34}S (4.29%). The TPD curve at *m/z* 68 does not contain a peak at 178 K, indicating that this peak is probably not due to S_2. The broad peak at 230 K is present in both TPD curves of *m/z* 68 and 64. The feature at 230 K may be primarily due to S_2 desorption. Considering all temperatures, we conclude that the signal at *m/z* 64 corresponds to at least S_2 and SO_2 contributions.

S_2 was reported as a UV photochemical product of H_2S–H_2O ice mixture (Jimenez-Escobar & Caro 2011) and X-ray irradiation of pure H_2S with a relatively high ratio $[S_2]/[H_2S]$ equaling 0.16 (Jimenez-Escobar et al. 2012). S_2 could be formed by several mechanisms in our irradiation experiment "with H_2S." S_2 could be a product of a reaction between two HS radicals (which are products of irradiation of H_2S), via the reaction $HS+HS \rightarrow H_2+S_2$, or could form in a reaction between atomic sulfur atoms via the reaction $S+S \rightarrow S_2$. In addition, OCS formed by irradiation could subsequently react with a sulfur atom and produce the sulfur dimer: $S+OCS \rightarrow S_2+CO$. Finally, S_2 could also be produced by dissociation of H_2S_2. While H_2S_2 was not originally reported in Mahjoub et al. (2016), we will report the possible detection of this molecule in our samples by IR spectroscopy later in this section.

In Figure 1(b) the comparison between TPD curves of "with H_2S" and "without H_2S" samples at *m/z* 80 indicates a sulfur-

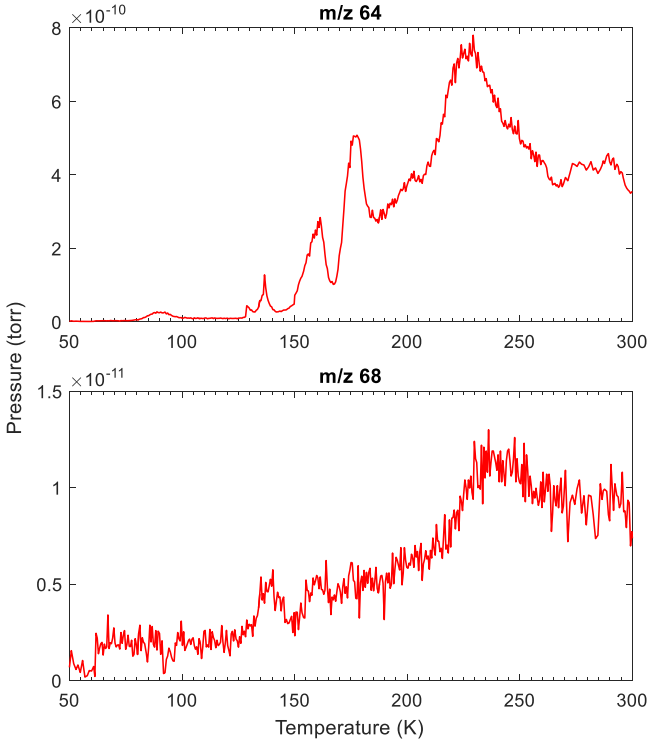

Figure 3. Comparison between TPD spectra at *m/z* 64 and *m/z* 68.

containing molecule. The sulfurous compounds that could be responsible for mass 80 are S_2O and SO_3. The principal fragment from both SO_3 and S_2O is SO (*m/z* 48). As discussed above, the signal at *m/z* 48 could derive from SO released from the ice via fragmentation of SO_2, SO_3, and S_2O, as well as CH_3SH. This hinders the identification of SO_3 and S_2O using the fragmentation pattern. Moreover, the signal at mass 84 ($^{34}S_2O$) is very weak and does not allow confirmation of the formation of S_2O. Irradiation experiments using isotopes labeled H_2S are needed to infer whether both SO_3 and S_2O contribute to the signal at mass 80. Both $SO_3$and S_2O have been produced in electric discharge applied to SO_2 (Hopkins et al. 1973). SO_3 was also observed as a product of ion bombardment of SO_2pure ice (Gomis & Strazzulla 2008).

Figures 1(c) and (d) of *m/z* 96 and 128 both peak in desorption around $T = 282$ K. We assign these two masses to the allotropes S_3 and S_4, respectively. S_3 is detected in irradiated H_2S (Jimenez-Escobar & Caro 2011). The desorption behavior observed at *m/z 96* is similar to S_3 after UV irradiation of pure H_2S (Jimenez-Escobar & Caro 2011), with a single peak between 250 and 300 K. Tetrasulfur, S_4, can be formed during co-deposition of S_2+Kr, forming a red film. Films of S_2 in Kr also form S_4 when irradiated with visible light (Meyer & Stroyerh 1972). Hassanzadeh & Andrews (1992) ruled out the formation mechanism of S_4 by recombination of two S_2 molecules in gas phase, but this reaction is possible in a matrix surface (Hopkins et al. 1973), which explains the formation of S_4 in co-deposited S_2–Kr mixture. Another reaction pathway could be: $S+S_3 \rightarrow S_4$. S_3 and S_4 have been detected as a product of electric discharge in gaseous SO_2 (Hopkins et al. 1973).

Sulfur allotropes S_2, S_3, and S_4 have very weak infrared absorption bands at wavenumbers between 200 and 600 cm^{-1}. This makes their detection in our samples by IR spectroscopy very difficult at low column densities.

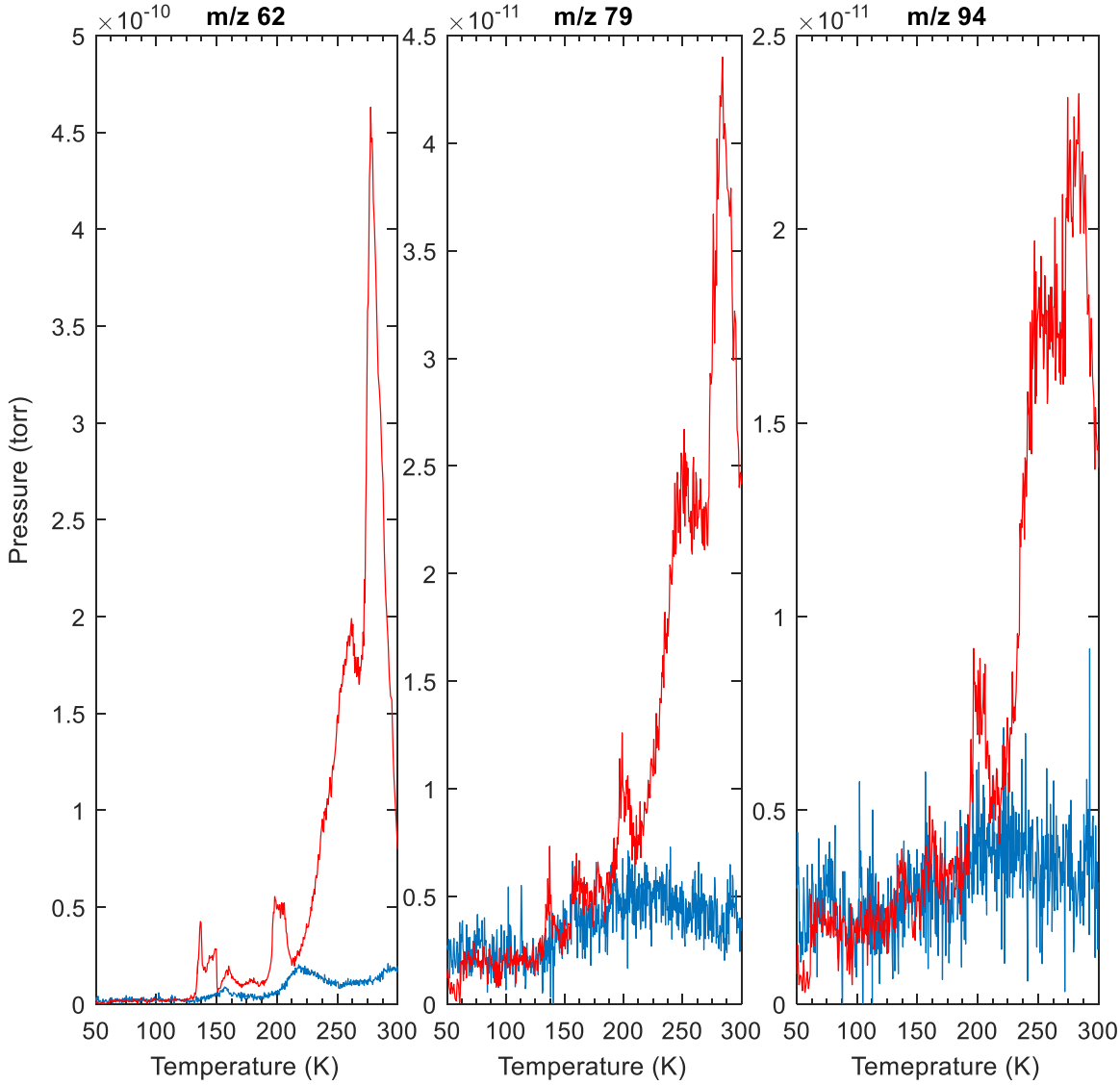

Figure 4. TPD curves corresponding to the irradiated "with H_2S" (red curves) and "without H_2S" (blue curves) experiments. Ion currents at *m/z* 62 and 94 correspond, respectively, to CH_3SCH_3 and $CH_3S_2CH_3 + CH_3SO_2CH_3$, *m/z* 79 assigned their principal fragments to $CH_3S_2 + CH_3SO_2$.

It is noteworthy that we did not detect any chains containing more than four S atoms in our TPD spectra, in spite of scanning to *m/z* 200 (S_5 and S_6 have molar masses of 160 and 192, respectively, while those of S_7 and S_8 are 224 and 256, which are beyond our range). The non-detection in the RGA mass spectrometer of sulfur allotropes higher than S_4 indicates that the signal corresponding to S_2, S_3, and S_4 could not be due to fragments of higher sulfur chains. This absence of sulfur chains in the mass spectra does not rule out the formation of S_x polymers ($x > 4$). These larger polymers like S_8 are less volatile, and if they were produced they likely remained in the organic residue left on the substrate at room temperature. A future study of the residue may clarify whether larger sulfur polymers do form by irradiation.

In addition to short sulfur chains we detected other organo-sulfur molecules (i.e., $C_xH_yS_z$). Figure 4 shows peaks at *m/z* 62 and 94 that provide evidence for the production of other sulfur-containing compounds. Mass 62 could be assigned to CH_3SCH_3. This assignment is supported by the detection of fragment CH_3S (*m/z* 47) of C_2H_6S at $T \sim 290$ K. The ratio of signal 62/47 at this temperature is 1.17, close to the ratio of signal 62/47 = 1.05 by electron impact mass spectrometry of CH_3SCH_3 (NIST Mass Spectra Data Center & Stein 2008). We cannot totally exclude the contribution of H_2COS (sulfine) to the signal detected at *m/z* 64, though sulfine is unstable and has a very short lifetime (Arnaud et al. 1999). Mass 94 could be assigned to CH_3–SO_2–CH_3 (dimethyl sulfone) and/or CH_3–S_2–CH_3 (dimethyl disulfide). Both molecules have a fragment at mass 79 (NIST Mass Spectra Data Center & Stein 2008). We have detected a signal at *m/z* 79 exclusively in the "with H_2S" sample (Figure 4). A close comparison between TPD spectra at 79 and 94 shows a ratio 79/94 $\sim$ 1.4 at $T = 255$ K and $\sim$1.9 at 284 K. The 79/94 ratios in NIST mass spectra of $CH_3SO_2CH_3$ and CH_3–S_2–CH_3 are, respectively, $\sim$2 and 0.57. The ratio 79/94 of $CH_3SO_2CH_3$ is fairly in agreement with the peak at 284 K, consistent with this desorption peak being dominated by dimethyl sulfone. The peak at 255 K could not be explained by $CH_3SO_2CH_3$ alone, so we tentatively assign this peak to the desorption of both CH_3–S_2–CH_3 and $CH_3SO_2CH_3$. The detection of large organo-sulfur molecules indicates that a complex carbon–sulfur chemistry is driven by irradiation of simple methanol-hydrogen-sulfide-containing ices. H_2S may have affected the

Table 1
Summary of Sulfurous Species Detected by Comparing TPD Measurements of Samples "with H_2S" with Samples "Without H_2S"

Mass	Assignment	T (K) of Principal Desorption Peaks
62	CH_3SCH_3, H_2CSO?	260, 278
64	S_2, SO_2	163, 179, 230
80	S_2O?, SO_3?	245, 290
94	$CH_3SO_2CH_3$, $CH_3S_2CH_3$	255, 284
96	S_3	282
128	S_4	282

Note. The question mark stands for possible assignment.

carbon chemistry in the sample by involving radicals and ions formed by irradiation of CH_3OH in sulfur-related chemical reactions. In addition to the possible effect of this chemistry on the colors of the irradiation residue, this chemistry could be astrobiologically relevant because of its role in the generation of diverse organic species. Detected species are summarized in Table 1.

Figure 5 shows IR spectra of samples "with H_2S" before and after irradiation. After two hours of irradiation, a band appears at 2507 cm^{-1}. One possible assignment of this band is the H_2S_2 dimer or H_2S_2–H_2S complex, based on previous assignments by Isoniemi et al. (1999). The S–H stretching mode of H_2S_2 is in the same position as the H_2S band (in the mixture H_2S–H_2O) at 2550 cm^{-1}, precluding direct detection of H_2S_2. This assignment needs to be definitively confirmed by isotopic effect studies. H_2S_2 could be produced by a reaction between two HS radicals. The maximum of the 2507 cm^{-1} band appears after two hours of irradiation, after which further irradiation decreases this band. At the end of the experiment (after 19 hr of irradiation) this band disappears completely. H_2S_2 formed early in the irradiation is likely dissociated by the irradiation and may react to form larger molecules. Isoniemi et al. (1999) studied UV photolysis of H_2S_2 ice in an Ar matrix and concluded that this photochemistry leads to the formation of the HS_2 radical and S_2. Dissociation of H_2S_2 presumably contributes to the production of S_2 detected by TPD. The infrared band strength of H_2S_2 is not reported in the literature, which prohibits the determination of the column density of H_2S_2 produced in our experiment.

4. Discussion

4.1. Applications to Jupiter Trojans and KBOs

This work aims to test the hypothesis correlating the color bimodality in Jupiter Trojans and small KBOs with the sulfur chemistry in the early solar system (Wong & Brown 2016). S_x chains have been considered as possible candidate sources of the coloring on the surface of Io (Nelson & Hapke 1978; Spencer et al. 1997), as well as the Great Red Spot of Jupiter. Organic macromolecules produced by irradiation of carbon- and nitrogen-containing ices are also proposed to explain the red slopes observed on the surfaces of small icy bodies. Sulfur small chains have the particularity of changing colors when submitted to thermal or irradiation processing. As explained in the review of sulfur color properties in the introduction, this color change is a function of the size of the sulfur polymer. This particularity could explain the difference between the colors of Trojans and KBOs. It is important to clarify that we are not claiming here that sulfur chains are alone responsible

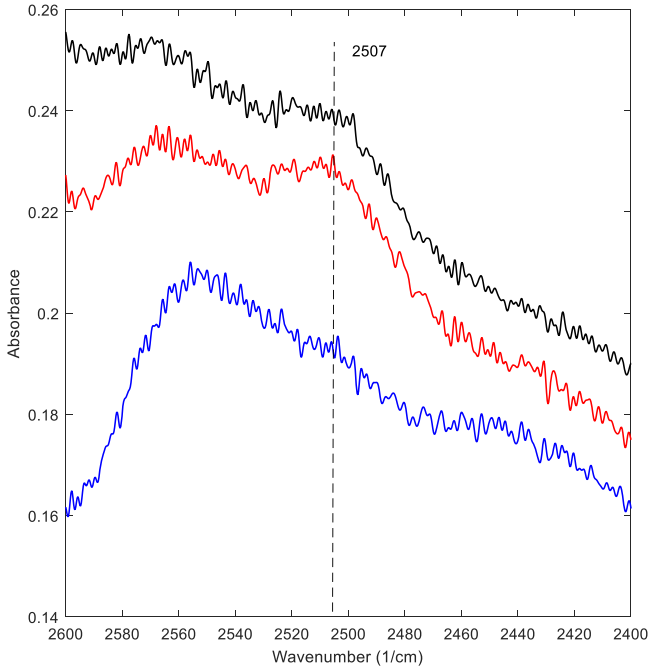

Figure 5. Infrared spectrum around 2550 cm^{-1} of the sample "with H_2S" before (blue), after 2 hr (red), and after 5 hr (black) of electron irradiation. The band at 2507 cm^{-1} is assigned to an H_2S_2 dimer. This band appears after 2 hr of electron irradiation (red) and decreases significantly after 5 hr (black).

for the spectral colors of Trojans and KBOs. An accurate estimation of the production rates of these species by irradiation and measurements of their quantitative optical properties (refractive indices) is needed to quantitatively estimate their role as coloring agents.

In the framework of the hypothesis that sulfur irradiation chemistry plays a key role in the color bimodality observed in KBOs and Trojans, our experimental work supports some aspects of the hypothesis:

1. Our laboratory simulations show that sulfur allotropes are produced as a result of electron irradiation of H_2S-containing mixed ices. It is conceivable that these sulfur materials bring about the red slope observed in Trojans and KBOs.
2. Stored at very low temperatures (~30, 50 K) and in a relatively low irradiation environment, KBOs are expected to preserve unstable small sulfur allotropes. Jupiter Trojans, on the other hand, are exposed to higher irradiation and a warmer environment. The thermal and irradiation processing experienced by Trojans in their migration pathway (as predicted by Nice model) can turn small red allotrope sulfur chains into neutral S_8. This is consistent with KBOs being redder than Trojans.

On the other hand, our results rebut one important prediction of that hypothesis:

1. VR KBOs are known to be much brighter than R KBOs and Trojans. Yellow sulfur polymers have a higher albedo compared to samples rich in small sulfur allotropes (like liquid sulfur). Therefore, the transformation of sulfur allotropes into large sulfur polymers could not explain the lower albedo of Trojans.

Detection of these molecules with remote sensing methods from telescopes and spacecraft would be challenging, but is not

unfeasible. Sulfur allotropes have very weak absorption bands in the far- and mid-IR regions, so they cannot be directly detected by remote infrared spectroscopy. However, these species have intense bands in the ultraviolet and visible ranges: S_2 absorbs from the ultraviolet to 500 nm or greater, with the band center occurring at 360 nm (Meyer & Stroyerh 1972; Steudel & Eckert 2003); S_3 has a broad absorption band centered at about 400 nm and extending to ~500 nm; and S_4 has a band centered at about 530 nm, an absorption between 460–590 nm that is attributed to the C_{2v} isomer, and a weaker band at 625 nm (Meyer & Stroyerh 1972). The molar extinction coefficient of S_3 is $\sim 10^{-16}$ cm^2 at 400 nm and is one order of magnitude higher than of S_4. Detection of these species by UV and Vis spectroscopy might be possible if they are present with measurable quantities. UV measurements of Trojans and KBOs are rare. (Stern et al. 2014) reported the only UV measurements of KBOs other than Pluto using the *Hubble Space Telescope*. They reported a UV absorption feature in the spectrum of KBO Haumea centered near 305 nm. They proposed SO_2 and OH as possible candidates for this band. Similar observations in the UV and high-quality spectra in the visible of other KBOs are needed to better constrain the presence of sulfur allotropes on the surface of these objects.

4.2. Sulfur Irradiation Products in Cometary Materials

With the exception of $C_2H_6S_2$ and $C_2H_6SO_2$, the list of sulfurous molecules detected in our experiment either by TPD in this paper or by FTIR spectroscopy (Mahjoub et al. 2016) matches exactly the list of sulfur molecules detected by the ROSINA/DFMS mass spectrometer at 67P (Calmonte et al. 2016). Disulfur, S_2, is ubiquitous in comets. This molecule was first detected in the UV spectra of comet C/1983 H1 (Ahearn et al. 1983). Since then, S_2 has been identified in many comets (Swamy & Wallis 1987; Laffont et al. 1998; Kim et al. 2003). Recently the ROSINA mass spectrometer on board the *Rosetta* spacecraft detected S_2 at a distance of 3.15 au from the Sun, with an abundance of $\sim 10^{-5}$ compared to water (Le Roy et al. 2015). Ahearn et al. (1983) suggested that S_2 comes from (or is formed very close to) the comet nucleus rather than by gas phase chemistry in the cometary coma. Indeed, S_2 is observed at distances larger than 3 au, where the gas density is very low and collisions are rare, these conditions are not convenient for gas phase recombination reactions. S_3 and S_4 have also been recently detected in the coma of comet 67P by the ROSINA/DFMS mass spectrometer on board the *Rosetta* spacecraft, and may originate from dust grains (Calmonte et al. 2016). The organo-sulfur molecule C_2H_6S has also been detected in the 67P coma (Calmonte et al. 2016), and the C_2H_6S/H_2S ratio is estimated to be around 10^{-4}. Calmonte et al. (2016) discussed the likelihood of radiolysis of H_2S in the pre-solar cloud as an origin of sulfurous molecules (particularly S_2). While our experiment does not depict the conditions of the pre-solar nebula, our work shows that radiolysis of ice mixtures containing CH_3OH and H_2S reproduces much of the list of sulfur species detected by *Rosetta*.

5. Conclusion

We present in this article a TPD study of irradiated CH_3OH–NH_3–H_2O ("without H_2S") and H_2S–CH_3OH–NH_3–H_2O ("with H_2S") ices. Small sulfur allotropes (S_2, S_3, S_4) are susceptible to being formed in the mixture "with H_2S," as well as more complex H_2S_2 and $C_xH_yS_z$ species. These sulfur polymers could characterize objects formed outside the stability line of H_2S and could play a role in the color of KBOs. Produced allotropes become unstable under irradiation and heating conditions, as would be experienced by an object scattered from the primordial KBO reservoir region (beyond 15 au) to the current Jupiter Trojans location. The small allotropes could convert into larger polymers, principally S_8, characterized by neutral spectra at wavelengths higher than 500 nm. This may flatten the red slope in the spectral reflectance of these objects. While these results support the chemical credibility of the hypothesis of a H_2S role in the color bimodality of Trojans, they are not able to explain some characteristics, such as the high albedo of KBOs compared to Trojans and the lack of absorption bands at visible wavelengths.

The main outcome of this laboratory work is the production and characterization of sulfur compounds that would be fingerprints left after irradiation of an object formed beyond the sublimation line of H_2S.

This work was conducted at the Jet Propulsion Laboratory, Caltech, under a contract with the National Aeronautics and Space Administration (NASA) and at the Caltech Division of Geological and Planetary Sciences. This work was supported by the Keck Institute of Space Studies (KISS).

We would like to thank the anonymous reviewer for pertinent comments that considerably improved the manuscript.

U.S. Government sponsorship is acknowledged.

ORCID iDs

Ahmed Mahjoub https://orcid.org/0000-0003-1229-5208
Michael E. Brown https://orcid.org/0000-0002-8255-0545
Bethany L. Ehlmann https://orcid.org/0000-0002-2745-3240
Kevin P. Hand https://orcid.org/0000-0002-3225-9426

References

Ahearn, M. F., Feldman, P. D., & Schleicher, D. G. 1983, ApJL, 274, L99
Arnaud, R., Juvin, P., & Vallee, Y. 1999, J Org Chem, 64, 8880
Baklouti, D., Schmitt, B., & Brissaud, O. 2008, Icar, 194, 647
Bennett, C. J., Pirim, C., & Orlando, T. M. 2013, ChRv, 113, 9086
Brabson, G. D., Mielke, Z., & Andrews, L. 1991, JPhCh, 95, 79
Brown, M. E., Schaller, E. L., & Fraser, W. C. 2011, ApJL, 739, 5
Calmonte, U., Altwegg, K., Balsiger, H., et al. 2016, MNRAS, 462, S253
Emery, J. P., Burr, D. M., & Cruikshank, D. P. 2011, AJ, 141, 18
Fraser, W. C., Brown, M. E., Morbidelli, A., Parker, A., & Batygin, K. 2014, ApJ, 782, 14
Gomis, O., & Strazzulla, G. 2008, Icar, 194, 146
Gradie, J., & Veverka, J. 1980, Natur, 283, 840
Hand, K. P., & Carlson, R. W. 2011, Icar, 215, 226
Hassanzadeh, P., & Andrews, L. 1992, JPhCh, 96, 6579
Hopkins, A. G., Tang, S. Y., & Brown, C. W. 1973, J Am Chem Soc, 95, 3486
Isoniemi, E., Pettersson, M., Khriachtchev, L., Lundell, J., & Rasanen, M. 1999, JPCA, 103, 679
Jimenez-Escobar, A., & Caro, G. M. M. 2011, A&A, 536, 11
Jimenez-Escobar, A., Caro, G. M. M., Ciaravella, A., et al. 2012, ApJL, 751, 5
Kim, S. J., Ah'earn, M. F., Wellnitz, D. D., Meier, R., & Lee, Y. S. 2003, Icar, 166, 157
Laffont, C., Boice, D. C., Moreels, G., et al. 1998, GeoRL, 25, 2749
Le Roy, L., Altwegg, K., Balsiger, H., et al. 2015, A&A, 583, 12
Mahjoub, A., Poston, M. J., Hand, K. P., et al. 2016, ApJ, 820, 9
Meyer, B. 1976, ChRv, 76, 367
Meyer, B., Oommen, T. V., & Jensen, D. 1971, JPhCh, 75, 912
Meyer, B., & Stroyerh, T. 1972, JPhCh, 76, 3968

Morbidelli, A., Levison, H. F., Tsiganis, K., & Gomes, R. 2005, Natur, 435, 462
Nelson, R. M., & Hapke, B. W. 1978, Icar, 36, 304
Nesvorny, D., Vokrouhlicky, D., & Morbidelli, A. 2013, ApJ, 768, 8
NIST Mass Spec Data Center, & Stein, S. E. 2008, in NIST Chemical WebBook, Standard NIST reference database Number 69, ed. P. J. Linstrom & W. G. Mallard (Gaithersburg, MD: National Institute of Standards and Technology), 20899 http://webbook.nist.gov
Quirico, E., Moroz, L. V., Schmitt, B., et al. 2016, Icar, 272, 32
Spencer, J. R., McEwen, A. S., McGrath, M. A., et al. 1997, Icar, 127, 221
Stern, S. A., Cunningham, N. J., & Schindhelm, E. 2014, AJ, 147, 6
Steudel, R., & Eckert, B. 2003, in Topics in Current Chemistry, ed. R. Steudel. (Berlin: Springer), 1
Swamy, K. S. K., & Wallis, M. K. 1987, MNRAS, 228, 305
Wong, I., & Brown, M. E. 2016, AJ, 152, 8
Wong, I., & Brown, M. E. 2017, AJ, 153, 9